Morphology and electronic properties of thermally stable TiO_x nanoclusters on Au(111)

Koen Lauwaet,* Koen Schouteden, Ewald Janssens, Chris Van Haesendonck, and Peter Lievens
Laboratory of Solid-State Physics and Magnetism & Institute for Nanoscale Physics and Chemistry (INPAC), Katholieke Universiteit Leuven, BE-3001 Leuven, Belgium

(Received 8 December 2010; revised manuscript received 24 February 2011; published 18 April 2011)

TiO_x clusters on atomically flat Au(111) films have been investigated by means of scanning tunneling microscopy and scanning tunneling spectroscopy. We present measurements of both the morphology and the electronic properties of these clusters. First, pure Ti clusters are produced in the gas phase and are deposited onto a clean Au(111) surface under controlled ultrahigh vacuum conditions. Next, the clusters are oxidized. Then, scanning tunneling microscopy measurements are performed before and after annealing up to high temperatures (970 K), indicating a high thermal stability of the deposited clusters. Scanning tunneling spectroscopy reveals an *n*-type semiconductorlike gap in the TiO_x cluster density of states. Local influence of the clusters on the electronic surface state of the Au(111) substrate is observed, which is relevant for catalytic cycles where certain steps of the cycles take place at the metal-oxide interface.

DOI: 10.1103/PhysRevB.83.155433 PACS number(s): 73.20.At, 36.40.Mr, 68.37.Ef, 68.43.Jk

I. INTRODUCTION

While the physical dimensions of clusters and nanoparticles are between those of individual atoms and molecules and bulk matter, their properties do not simply scale with the particle size. The transition from a single atom to the respective solid involves quantum size effects. Clusters reveal remarkable size-dependent electronic, structural, and magnetic properties, implying clusters have attracted considerable attention.[1]

Transition-metal particles and, in particular, TiO_2 clusters are of high fundamental and technological interest due to their optical, catalytical, and photocatalytical properties. The particles are being applied in various fields, including sunscreen agents,[2] removal of various types of aqueous pollutants,[3] and antibacterial and detoxification effects.[4] Information about the electronic structure of free Ti clusters has been obtained by performing core-level spectroscopy,[5] and by combining photoelectron spectroscopy with theoretical calculations.[6] Deposition of preformed TiO_x clusters has been performed[7–9] in order to study the properties of thick cluster assembled films. Both the final morphology and the optical gap of the films were shown to depend on the initial cluster size.[8,10]

In the case of individual particles on a surface, the morphology and electronic properties of a variety of nanoparticles have been investigated in detail in a controlled environment.[11–13] However, attempts to explore individual nanosized TiO_2 (titania) particles are scarce. Recently, TiO_x nanoparticles with x close to 2 have been grown by atomic evaporation of Ti onto thin layers of H_2O and NO_2 adsorbed on Au(111). The buffer layer subsequently was evaporated, resulting in the formation of various self-assembled TiO_x nanoparticles on the Au(111) surface.[14,15] The morphology of these particles strongly depends on the buffer layer and on the annealing temperature used in the growth process, and their crystal structure is typically that of rutile titania.[15] TiO_x particles are known for their high catalytic activity[16,17] and exhibit a highly temperature-dependent morphology.[14] Although clean Au(111) is not catalytically active for the water gas shift (WGS), gold surfaces that are 20% to 30% covered by titania nanoparticles have a catalytic activity comparable to, and even higher than, that of a good WGS catalyst such as Cu(100).[16] By interaction of H_2O and CO with TiO_x/Au(111), the water dissociates on oxygen vacancies of the titania and CO adsorbs on gold sites located nearby. Subsequent reaction steps, leading to the formation of CO_2 and H_2, take place at the metal-oxide interface. The interaction between TiO_x and Au(111) is supposed to play an important role in the catalytic activity because of cooperative effects at the oxide-metal interface.[16] For Au particles grown on TiO_2, it is known that there occurs a charge transfer from the defect sites of TiO_2 to the gold nanoparticle.[18] In the opposite case of TiO_x nanoparticles grown on Au(111), the presence of a similar charge transfer and its relevance for heterogeneous catalysis are still open questions.

In this paper, we report on the investigation of individual TiO_x nanoparticles on clean Au(111) created by deposition of preformed pure Ti clusters on a Au(111) surface, which are subsequently oxidized. The Ti clusters are preformed in the gas phase and are deposited with low kinetic energy onto single-crystalline flat surfaces. This alternative preparation route offers a high degree of freedom to tune the properties of nanostructured materials by selecting the appropriate particle size, composition, kinetic energy, and substrate.[19] Preformed clusters are grown and deposited under ultrahigh vacuum (UHV) conditions, allowing for the creation of clean and well-defined samples and ensuring to obtain particles that are immobilized on the Au(111) surface by strong Ti-Au bonds since no oxygen is present during the deposition of the particles.

The alternative preparation route enabled us to investigate the morphology as well as the electronic properties of nanometer-sized clusters consisting of a few up to several hundreds of atoms by means of scanning tunneling microscopy (STM) and scanning tunneling spectroscopy (STS) under controlled conditions. STM combined with STS offers the ideal means to study in detail, down to the atomic scale, both the geometrical and electronic properties of individual nanoparticles on metallic substrates. The influence of annealing on the cluster morphology was studied up to high

temperature (970 K). With STS, we probed the local electronic properties of the clusters as well as their influence on the surrounding Au(111). The possible relevance of our findings for the understanding of the catalytic performance of the TiO_x-Au(111) system is discussed.

II. EXPERIMENT

A. Substrate preparation

Epitaxially grown 140-nm thick Au(111) films on freshly cleaved mica were prepared *ex situ* by molecular beam epitaxy (MBE) at elevated temperatures.[20] After exposure to ambient conditions, the Au(111) surfaces are cleaned in the UHV preparation chamber (with a typical base pressure in the low 10^{-10} mbar range) of the low-temperature UHV STM by repeated cycles of Ar ion sputtering (at about 4 keV, 10^{-6} mbar of Ar pressure, and with the beam current density typically around 50 $\mu A/cm^2$) and annealing at about 720 K.[21] The resulting films consist of atomically flat islands with dimensions up to 500 × 500 nm^2. Substrates are then transported under vacuum first to the cluster deposition apparatus and after cluster deposition back to the STM setup by means of a home-built transport vessel (pressure in the 10^{-10} mbar range). The vessel consists of a small chamber equipped with a long transport arm and an ion pump that can run autonomously for 24 hours using a battery.

B. Cluster production and deposition

Ti clusters were produced by a laser vaporization source,[22] which is connected to a UHV cluster deposition chamber with a base pressure below 5×10^{-10} mbar.[20] Cluster beams with a size distribution ranging from a few atoms up to several hundreds of atoms can be produced, as recorded with time-of-flight mass spectrometry. A typical mass spectrum of the free cationic Ti clusters as a function of (a) the number of atoms in the cluster and (b) the corresponding cluster diameter is presented in Fig. 1. The diameter was calculated assuming the clusters to be spherical and using the Wigner-Seitz radius for Ti (0.17 nm, see Ref. 23). The maximum in the cluster-size distribution was tuned to around 750 atoms (≈3.1 nm cluster diameter). We note, however, that clusters larger than those observed in the mass spectra may be present in the cluster beam since the measured cluster distribution has an upper cutoff due to the decreasing efficiency of the detector for the largest clusters. The clusters were deposited with their inherent low kinetic energy (≈0.13 eV/atom) onto cleaned Au(111) substrates at room temperature. This kinetic energy is small when compared to the atomic binding energy within the cluster and, consequently, negligible cluster fragmentation is expected upon impact. Deposition times were chosen to achieve a low coverage of clusters on the substrate, i.e., well below one monolayer. There is a quartz microbalance installed to monitor the film thickness. Ti clusters can be made with a very low oxygen content (a few atoms per cluster), as observed in experiments on free Ti clusters.[5,9] This ensures that the bond between the Au(111) and the Ti cluster will be formed by the pure metals.

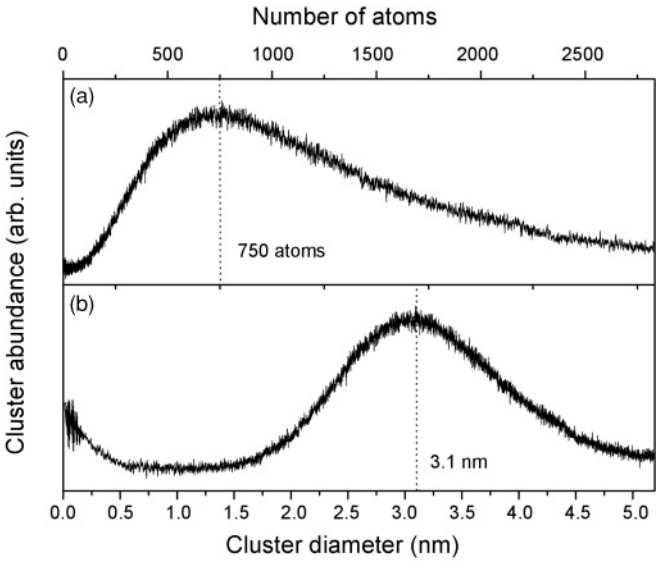

FIG. 1. Abundance spectra of free cationic Ti clusters as a function of (a) the number of atoms in the cluster and (b) the corresponding cluster diameter. The mean cluster size was tuned to be around 750 atoms (≈3.1 nm cluster diameter). The cluster diameter was calculated assuming a spherical shape.

C. Oxidation

Oxidation of the deposited clusters is achieved by lowering the vacuum conditions in the transport vessel. For this purpose, we switched from ion pumping to pumping with a turbomolecular pump. This way, the vacuum is kept in the 10^{-7} mbar range for a few minutes. When analyzing the gases present in the vacuum chamber with a mass spectrometer, the highest partial pressures were found for O_2 (8×10^{-8} mbar) and H_2O (4×10^{-7} mbar), with only a low background pressure of hydrocarbons (10^{-9} mbar range). Under these conditions, the Ti clusters interact with both O_2 and H_2O to form titanium oxide.[14] We can not, however, fully exclude that a small amount of hydroxyl groups is adsorbed on the Ti surface as well.[14] It is known that oxide can penetrate up to 5 nm into the surface of Ti films, implying that the clusters investigated here may be (nearly) completely oxidized.[24] From previous experiments using reactive sputtering of Ti with an oxygen-rich plasma, it is known that, instead of stoichiometric TiO_2, an oxygen-deficient TiO_x phase with x close to 2 is formed.[25]

D. Low-temperature UHV STM and STS

All measurements were performed with a low-temperature UHV STM (Omicron NanoTechnology) at liquid-helium (4.5 K) or liquid-nitrogen (77.8 K) sample temperature and a base pressure in the 10^{-11} mbar range. Both mechanically cut and preformed PtIr (10% Ir) tips were used, as well as electrochemically etched W tips. The latter were cleaned *in situ* by repeated flashing at high temperature in order to remove the oxidized surface layer and additional contamination. The known electron surface state of the Au(111) surface at −480 meV was used as a reference for tip quality during our STS measurements.[26] STM topographic imaging was performed in constant current mode. I and V correspond to

the tunneling current and voltage, respectively. Differential conductance images, referred to as maps of the local density of states (LDOS) hereafter, are acquired with a closed feedback loop by means of harmonic detection with a lock-in amplifier at modulation frequencies in the 700–1500 Hz range and modulation amplitudes in the 30–60 mV range. Additionally, $I(V)$ curves are locally recorded with an open feedback loop, from which $dI/dV(V)$ curves are numerically calculated. The bias voltages indicated in text and figure captions are with respect to the sample. The STM tip is virtually grounded. Image processing was performed by Nanotec WSxM.[27] Annealing the clusters after deposition was done in different steps at increasing temperatures ($\Delta T \approx 50$ K) for about 12 hours per step in the UHV preparation chamber of the STM, starting at 420 K.

III. RESULTS AND DISCUSSION

A. TiO_x clusters on Au(111) after deposition

Figure 2(a) presents a typical STM image of TiO_x clusters on an atomically flat Au(111) surface before annealing. Particles of various lateral sizes and with different heights are retrieved on the surface. The particles are randomly distributed across the surface. Some contamination was observed on the Au(111) substrate after Ti cluster deposition and oxidation (less than one monolayer). This contamination leads to a roughening of the substrate as seen in Figs. 2(a) and 2(b). Locally, the atomically flat Au(111) surface can still be discerned [Fig. 2(a) on the left-hand side]. Reaction of TiO_x with excess oxygen leads to oxygen spillover from titanium nanoparticles to the gold surface, possibly explaining the observed contamination on the Au(111) surface.[28]

The amount of TiO_x nanoparticles retrieved on the surface is around 20 per 100 nm^2 and agrees well with the amount of deposited clusters estimated from measurements with the quartz microbalance (24 clusters per 100 nm^2). The TiO_x nanoparticles are distributed randomly across the Au(111) surface and do not show any preferential positioning at, e.g., Au(111) step edges, nor do they show any clear alignment at elbows of the Au(111) reconstruction as was the case for self-organized Co islands in a previous study.[13] These findings imply that the TiO_x nanoparticles do not exhibit significant diffusion on Au(111) at room temperature.

The height distribution of the particles after deposition is presented in Fig. 2(c). When measuring with STM, the particle height should equal the diameter of the free cluster provided it remains spherical upon deposition. In case the clusters flatten out and become hemispherical, the height of the particle should equal the radius of a hemisphere having the same volume of the free cluster. Figure 2(c) includes an abundance spectrum of the free cationic TiO_x clusters in the gas phase, both as a function of cluster diameter in the spherical approximation (d_s, gray) and as a function of cluster radius in the hemispherical approximation (r_h, black). They relate to each other as $r_h = 2^{-2/3} d_s$. Comparison of the abundance spectra with the height distribution of the TiO_x clusters clearly reveals that the deposited clusters can be considered as individual hemispherical particles after deposition. This result is similar to what is observed for deposited Co clusters on Au(111).[13] The observed cluster height is used to determine the flattening of the particles. The observed broadening can not be used since, with STM, the width of the particles can not be accurately measured due to the finite size of the tip.[13] Below, we demonstrate that there occurs a strong interaction between the TiO_x clusters and the Au(111) surface, which can account for this flattening. In contrast to Co clusters on Au(111),[13] the height histogram of the TiO_x nanoparticles on Au(111) does not reveal preferential cluster heights. This conclusion should be considered with care because of the uncertainties in the height determination that are caused by the contaminants. The contaminants can be moved by the tip while scanning, leading to an increased uncertainty on the height determination of

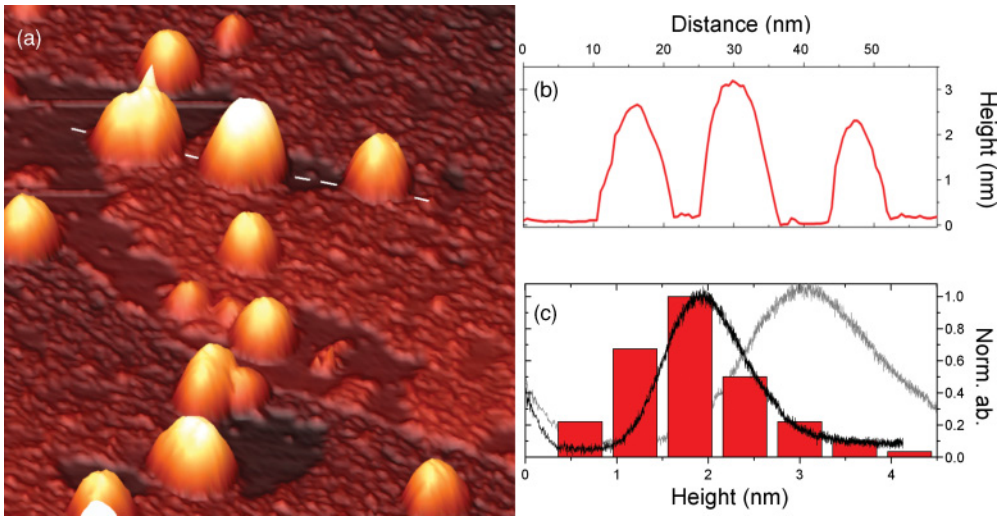

FIG. 2. (Color online) (a) 100 × 100 nm^2 STM image of deposited TiO_x clusters on a Au(111) surface ($V = 1.0$ V, $I = 1.0$ nA). The clusters show negligible mobility after deposition. (b) Height profile taken along the dashed white line in (a) comprising three TiO_x clusters. (c) Normalized height histogram of the deposited TiO_x clusters and complementary abundance spectra of free cationic TiO_x clusters as a function of cluster diameter in the spherical approximation (gray) and as a function of cluster radius in the hemispherical approximation (black).

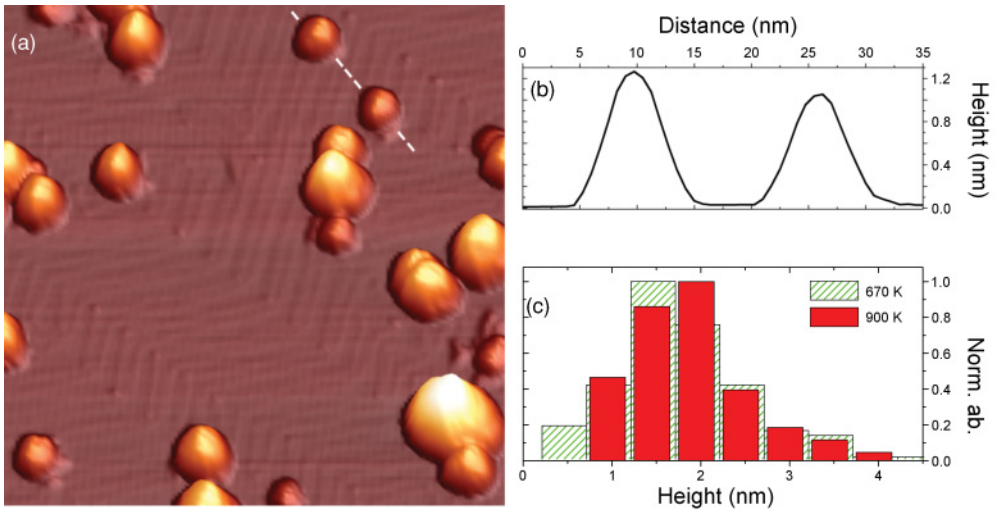

FIG. 3. (Color online) (a) $100 \times 100\,\mathrm{nm}^2$ STM image of TiO_x nanoparticles on a Au(111) surface after annealing to 970 K ($V = -1.0$ V, $I = 0.1$ nA). (b) Line profile taken along the dashed white line indicated in (a). (c) Normalized height histogram of the TiO_x nanoparticles after annealing to 670 K (dashed) and after annealing to 970 K (shaded).

around 0.2 nm. Detailed STS measurements are hampered as well by this layer.

B. Influence of annealing to elevated temperatures

In a next step, we have performed a systematic investigation of the influence of annealing the sample, following the procedure described in Sec. II D. Figure 3(a) presents a topographic STM image after annealing of the TiO_x nanoparticles up to a temperature of 970 K. Comparison with Fig. 2(a) shows that the substrate is now atomically flat and the Au(111) herringbone reconstruction is observed, indicating a clean surface. The contamination layer is evaporated, which happened already after annealing to 570 K (data not shown). The removal of this layer also eliminates the uncertainty for the height measurement. Still, no preferential cluster heights are observed when looking at an ensemble containing a lot of different clusters.

Analysis of the STM images after annealing to 670 and 970 K does not reveal a significant difference in the distribution of particle heights [Fig. 3(c)] when compared to the substrate before annealing [Fig. 2(c)]. This indicates that TiO_x nanoparticles do not "sink" into the Au(111) surface as is the case for, e.g., Co nanoparticles.[29] Meanwhile, the density of particles on the surface also remains constant (around 20 per 100 nm^2). After annealing, the particles are still randomly distributed across the surface and they do not coalesce. From these results, it can be concluded that, even at high temperatures, the TiO_x nanoparticles do not diffuse and remain on the surface as single entities. The maximum applied annealing temperature (970 K) is higher than the temperature used for annealing of the gold film after Ar bombardment (720 K). At 720 K, Au atoms are able to diffuse on a clean Au(111) surface to a degree that even nanosized islands and vacancies are able to flatten out.[30] However, after depositing the TiO_x nanoparticles on the Au(111), no additional changes of the Au(111) surface are observed up to 970 K.

A similar annealing procedure was followed by Osgood *et al.* in order to investigate the evolution of TiO_x nanoparticles created by atom deposition after H_2O adsorption on Au(111).[14] The TiO_x nanoparticles in the cited study showed a clear evolution, i.e., coagulation of particles, leading to an increased particle size after annealing to 300, 500, and 700 K. Our annealing temperature of 970 K is higher than 700 K, but, nevertheless, we do not observe any significant changes in substrate morphology. TiO_x nanoparticles grown by deposition of Ti clusters on Au(111), which are subsequently oxidized, therefore have an enhanced stability when compared to their counterparts grown by atom deposition on H_2O.

One could question if the thermal stability can be explained by bonding of the clusters to defects in the surface. Previous experiments on Ag clusters deposited on graphite demonstrated that mobile clusters can be captured and stabilized by surface defects.[31] The Au(111) surface contains intrinsic defects at the elbows of the herringbone reconstruction.[32] However, in Fig. 3(a), one can spot clusters that are not located at elbow sites of the Au(111) surface reconstruction after annealing (e.g., the upper cluster on the dashed white line). Stability of these clusters can, therefore, not be attributed to intrinsic surface defects present under the clusters.

Another possibility is that the clusters create their own defects in the gold surface upon landing. When cluster deposition is done with low kinetic energy, we do not expect that defects are created upon deposition.[33] In the case of deposition of, e.g., Ag clusters on graphite, the required energy for "self-pinning" due to defect creation is 10.4 eV/atom.[34] This value is significantly higher than the 0.13 eV/atom used in our experiments and, hence, no surface damage is expected. Therefore, surface defects can not explain the stability of our clusters.

The low mobility of the clusters on the Au(111) surface can be explained by the growth process of the TiO_x nanoparticles. The clusters made in the gas phase consist of metallic Ti, ensuring upon landing available atoms to form Ti-Au bonds. The bond between Au and Ti is known to be strong, i.e., 2.5 eV

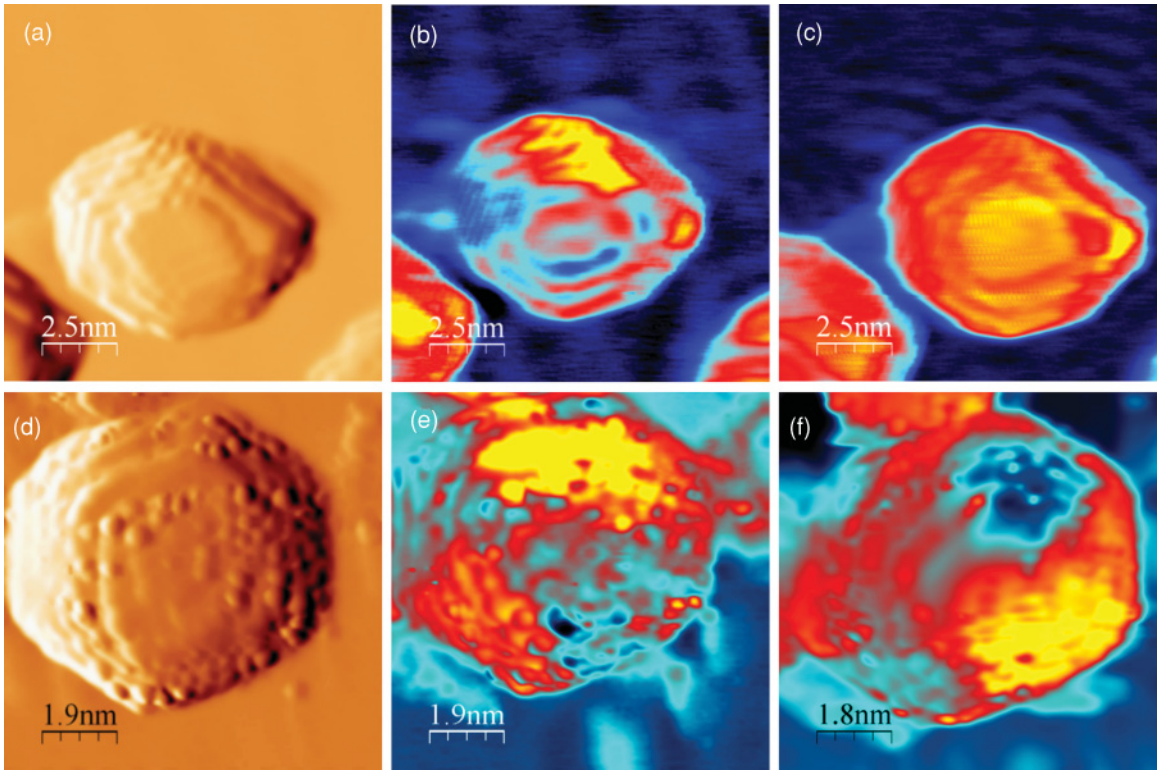

FIG. 4. (Color online) (a), (d) 12 × 12 nm^2 and 10 × 10 nm^2 derivatives of the STM images of two TiO_x clusters on Au(111) after annealing to 700 K ($V = +600$ mV, $I = 0.3$ nA). (b), (e) Corresponding LDOS maps taken at −600 meV. (c), (f) Corresponding LDOS maps taken at +600 meV. (c) Reveals the formation of standing wave patterns at the Au(111) surface due to scattering of Au surface state electrons at the TiO_x cluster.

for the diatomic species,[35] compared with 2.3 eV for diatomic gold[35] and 1.5 eV for diatomic titanium.[36] Once oxidized, the oxygen will prevent the Ti from diffusing into the Au substrate during the annealing process, as would happen in the case of pure Ti nanoparticles.[37,38]

Next, we zoomed in on individual clusters. Two typical results are presented in Figs. 4(a) and 4(d). For reasons of clarity, the "derivative image" of the recorded topography image is shown.[27] One can discern that there are nanoparticles that exhibit a hexagonal shape on the gold. The nanoparticles seem to have a flat top and clearly defined steps (step height: 0.23 nm ± 0.03 nm). Our observations are consistent with previous experiments on TiO_2 nanoparticles formed on Au(111) by different methods, from which it was concluded that the hexagonal TiO_2 particles have a rutile crystal structure with their (100) plane oriented parallel to the Au(111) surface.[15,28] Similar hexagonal formations have been observed when TiO_2 nanoparticles are formed on Au(111) by different methods.[15,28] Figure 4(d) reveals the presence of "dots" on the cluster surface. Adhesion of molecular oxygen on the titanium surface is likely to cause such "dots" since similar features were observed after the oxidation of a titanium film under controlled conditions.[39]

C. Electronic properties of TiO_x nanoparticles on Au(111)

After annealing to 570 K, the layer of surface contamination is evaporated and stable spectroscopy can be performed. Figure 4(b) is a LDOS map taken at −600 mV on the cluster presented in Fig. 4(a). The step edges of the atomic layers of the nanoparticle stand out clearly in the LDOS map. These edges can also be observed in the LDOS map taken at +600 mV [Fig. 4(c)]. On clusters where the "dotlike" features are present [see Fig. 4(d)], the LDOS map is strongly affected by these "dots" [see Figs. 4(e) and 4(f)], indicating that the oxygen molecules locally disturb the electron density of the cluster. It is not surprising that we do not observe two-dimensional standing wave patterns on the uppermost facet of the cluster. The impurities will induce additional scattering of the electrons inside the cluster, and interference patterns purely defined by topography will be washed out. Part of the electron density in the TiO_x clusters is, however, still related to their topography since step edges stand out in the LDOS maps. Previous observations of the LDOS of deposited Co clusters also revealed a topological dependence.[13]

Upon careful inspection of the LDOS map of Fig. 4(c), it can be seen that interference patterns are present on the Au(111) surface surrounding the TiO_x cluster, which can be related to scattering of Au surface state electrons. As already discussed above, the clusters do not damage the Au(111) surface upon deposition, implying that surface defects can not explain the observed scattering of Au(111) surface electrons. We therefore conclude that the clusters act as a strong scatterer for Au surface state electrons, indicative of a strong interaction between the cluster and the Au(111) surface.

Typical $I(V)$ and corresponding dI/dV(V) spectra taken on a TiO_x nanoparticle and on the surrounding Au(111) are shown in Figs. 5(a) and 5(b), respectively. The nanoparticle

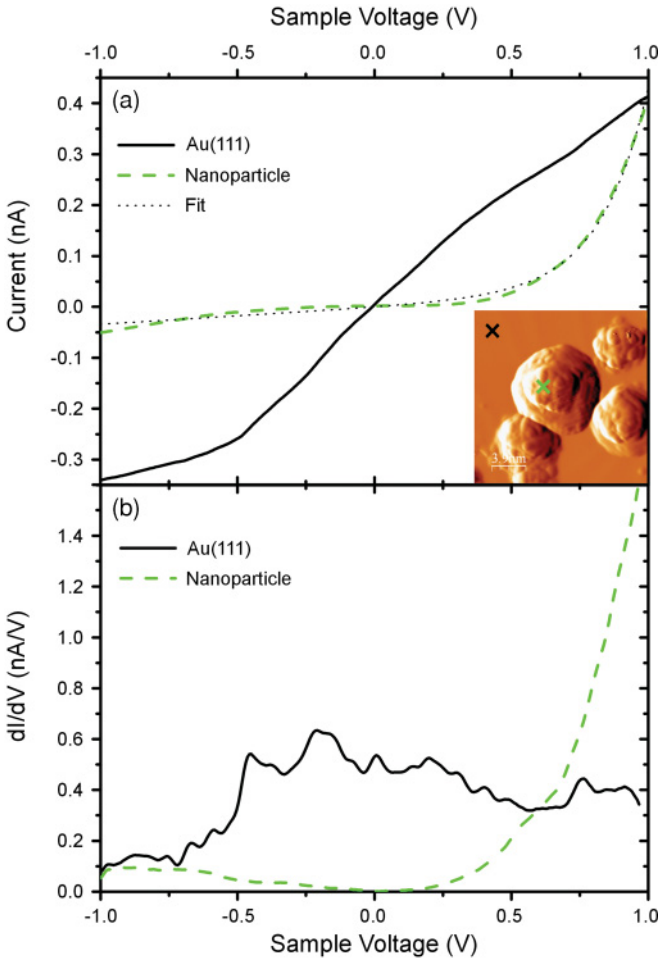

FIG. 5. (Color online) (a) $I(V)$ and (b) corresponding $dI/dV(V)$ spectra taken at the center of a TiO_x nanoparticle (dashed line) and at the surrounding Au(111) surface (solid line). Inset: $35 \times 35\ nm^2$ derivative of an STM image of the TiO_x cluster after annealing to 670 K ($I = 0.4$ nA, $V = 1.0$ V).

exhibits a rectifying *I(V)* behavior: the tunneling current is much higher for positive than for negative bias, where the current is nearly completely suppressed. This asymmetric *I(V)* behavior corresponds to that of a rectifying element in parallel with a leak resistor and can be described by $I(V) = a[\exp(\alpha V) - 1] + bV$, in which a is the current of the system for reverse bias, α denotes the ideality of the diode, and b corresponds to the inverse leak resistance of the system.[40] The latter can be related to an incomplete oxidation of the TiO_x cluster ($x < 2$). By fitting the equation to the experimental data [see Fig. 5(a)], we find that α is much larger than 1, which is typical for nanoscale diodes.[41,42]

It is known that nonstoichiometric TiO_x behaves as an n-doped semiconductor (the Fermi level is located near the conduction band).[43] Charge transfer hence takes place between the semiconducting TiO_x nanoparticle and the metallic Au(111), leading to the formation of a nanosized Schottky diode. Such charge transfer was previously reported for the opposite case of Au nanoparticles on TiO_2 substrates.[44] It must be noted that the amount of charge transfer depends strongly on the oxidation state of the nanoparticle.[45]

The formation of a Schottky diode indicates that oxygen is also present inside the nanoparticle and that the presence of oxygen is not limited to the dotlike features that are observed on the surface of the clusters [see Fig. 4(d)]. As already indicated above, it was shown that oxide can penetrate up to 5 nm into the surface of Ti films, implying that the clusters investigated here are (nearly) completely oxidized (x close to 2).[24] In addition, it is known from previous experiments that an oxygen content x of at least 1.35 is needed for TiO_x to become n-type semiconducting.[25] Nevertheless, formation of oxygen vacancies at the surface of the nanoparticles during annealing to elevated temperatures can be expected. This can be interesting in view of technological applications, since oxygen vacancies are essential for the catalytic behavior of the TiO_x-Au(111) system, e.g., for the WGS.[16] However, it was shown by Biener *et al.* that, for the case of TiO_x nanoparticles grown on Au(111) by Ti atom deposition, nonoxidized Ti diffuses into the Au(111) surface at elevated temperatures, while TiO_2 remains at the Au(111) surface.[28] Similar results have been reported more recently by Potapenko *et al.*[38] Within the resolution of our measurements, we do not observe any significant change of the cluster dimensions in our STM images as well as in our cluster-height histograms after annealing. We therefore conclude that the oxidation state of the TiO_x clusters is close to 2 and at least higher than 1.35.

Figure 6(b) presents a two-dimensional visualization of $dI/dV(V)$ spectra recorded along the white line crossing the cluster presented in the inset of Fig. 6(a). A so-called "tip state" occurs at 0.1 V in the dI/dV spectrum of the Au(111) surface presented in Fig. 6(a). Since this maximum does not

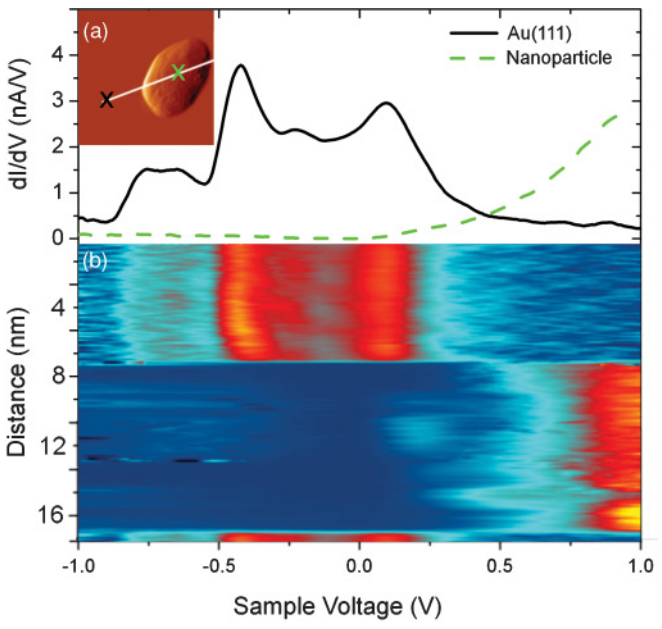

FIG. 6. (Color online) (a) dI/dV spectra at the center of a TiO_x cluster (dashed line) and at the surrounding Au(111) surface (solid line). Inset: $21 \times 21\ nm^2$ derivative of a STM image of this TiO_x cluster that has been annealed at 670 K. (b) Two-dimensional visualization of the dI/dV spectra along the white line in (a) shows the spatial dependence of the LDOS inside the cluster and the bending of the Au(111) surface state near the edge of the cluster ($I = 1.0$ nA, $V = 1.0$ V).

occur for other STM tips, it can be attributed to the presence of an electronic state localized at the apex of the STM tip. The cluster exhibits a clear gap in the DOS [dark region in the lower part of Fig. 6(b)] that varies across the cluster surface and is asymmetric about zero bias voltage.

When crossing from the cluster to the gold, atomically sharp transitions in the DOS are observed [at distances of 8 and 17 nm in Fig. 6(b)]. These abrupt transitions can be attributed to intrinsic tip switching. Whereas the atomically flat Au(111) surface as well as the top of the TiO_x clusters are probed by the outermost tip asperity, the cluster edges are probed by different asperities at both sides of the tip.[13] The "tip state" around 0.1 V is related to the outermost tip asperity and is therefore observed on the whole Au(111) surface in the dI/dV spectra in Fig. 6(b). On the Au(111), near the edges of the cluster, one can observe an influence of the nanoparticle on the Au(111) surface state: the onset of the surface state shifts toward higher energies (by about 80 meV) in the vicinity of the nanoparticle. The tip-related maximum at 0.1 eV remains constant as expected. The shift of the surface state at −480 meV can be attributed to a local electron transfer from the TiO_x nanoparticle to the Au(111) surface, resulting in a shift of the onset energy of the surface electrons. This result further supports the idea of the formation of a nanosized Schottky diode.

The modification of the electronic structure of the substrate close to deposited particles is a known phenomenon[44] and is of high importance for the catalytical activity of a system. On a metal that exhibits a surface state, stable molecules such as CO experience a strong Pauli repulsion due to the electrons stemming from the surface state.[46] The observed repression of the surface state around the nanoparticle leads to a lower Pauli repulsion and can lower the activation energy for dissociation of adsorbates significantly.[46] The observed shift of the Au(111) surface state near the edges of the cluster thus is relevant for the high catalytic activity of the TiO_x-Au(111) system. In particular, the high performance of the WGS reaction on TiO_x-Au(111) catalysts was shown to heavily rely on the direct participation of the metal-oxide interface.[16] The adsorption and dissociation of water takes place on the oxide, whereas the CO adsorbs on sites of the gold substrate located in the vicinity of the cluster. All subsequent steps to complete the catalytic cycle occur at the oxide-metal interface. In this context, the observed bending of the surface state near the cluster edges induces a preferential binding of the CO on the Au(111) surface in the cluster vicinity.[46,47] Next, the local charge transferred to the Au(111) surface from the TiO_x nanoparticle can be partially transferred to the CO molecules. Such charge transfer facilitates breaking of the molecular CO bond, thereby leading to reduced potential barriers for the reaction of CO with oxygen.[46,48] The cooperative effect between the TiO_x and the Au(111) surface thus can enhance the catalytic performance of the TiO_x-Au(111) system.

IV. CONCLUSIONS

The morphology and electronic properties of preformed Ti clusters deposited and subsequently oxidized on clean Au(111) under controlled UHV conditions were investigated before and after annealing up to high temperatures by means of STM and STS. By systematic analysis of the STM data, we demonstrated that the TiO_x clusters experience only a limited flattening resulting from the deposition and that their shapes can be approximated by hemispheres. A negligible mobility of the clusters on the Au(111) surface was observed upon annealing to temperatures as high as 970 K. After annealing, some of the nanoparticles are observed to exhibit hexagonal facets. STS measurements reveal that the clusters exhibit a rectifying behavior, which is attributed to the formation of a Schottky junction between the n-type semiconducting TiO_x clusters and the Au(111) surface. A charge transfer to the Au(111) substrate in the vicinity of the cluster was observed. This is relevant for the high catalytic activity of this system, since the charge transfer locally creates a preferential binding site for reagents on the Au(111) surface in the vicinity of the cluster and facilitates the activation of adsorbates. Both issues are essential for catalytic cycles where reaction steps take place at the metal-oxide interface.

ACKNOWLEDGMENTS

This research was supported by the Research Foundation-Flanders (FWO, Belgium) as well as by the Belgian Interuniversity Attraction Poles (IAP) and the Flemish Concerted Action (GOA) research programs. K.L. acknowledges the Institute for the Promotion of Innovation through Science and Technology in Flanders (IWT-Vlaanderen) for additional financial support, while K.S. acknowledges the FWO for additional financial support.

*Koen.Lauwaet@fys.kuleuven.be

[1] C. Binns, Surf. Sci. Rep. **44**, 1 (2001).
[2] A. Jaroenworaluck, W. Sunsaneeyametha, N. Kosachan, and R. Stevens, Surf. Interface Anal. **38**, 473 (2006).
[3] J. M. Herrmann, Catal. Today **53**, 115 (1999).
[4] K. Sunada, Y. Kikuchi, K. Hashimoto, and A. Fujishima, Environ. Sci. Technol. **32**, 726 (1998).
[5] P. Piseri, T. Mazza, G. Bongiorno, C. Lenardi, L. Ravagnan, F. Della Foglia, F. DiFonzo, M. Coreno, M. DeSimone, K. C. Prince, and P. Milani, New J. Phys. **8**, 136 (2006).
[6] M. Castro, S. R. Liu, H. J. Zhai, and L. S. Wang, J. Chem. Phys. **118**, 2116 (2003).
[7] F. Della Foglia, T. Losco, P. Piseri, P. Milani, and E. Selli, J. Nanopart. Res. **11**, 1339 (2009).
[8] M. C. Barnes, A. R. Gerson, S. Kumar, and N. M. Hwang, Thin Solid Films **446**, 29 (2004).
[9] I. Shyjumon, M. Gopinadhan, C. A. Helm, B. M. Smirnov, and R. Hippler, Thin Solid Films **500**, 41 (2006).
[10] E. Barborini, I. N. Kholmanov, A. M. Conti, P. Piseri, S. Vinati, P. Milani, and C. Ducati, Eur. Phys. J. D **24**, 277 (2003).
[11] K. L. Jonas, V. Von Oeynhausen, J. Bansmann, and K. H. Meiwes-Broer, Appl. Phys. A: Mater. Sci. Process. **82**, 131 (2006).

[12]A. Kleibert, F. Bulut, R. K. Gebhardt, W. Rosellen, D. Sudfeld, J. Passig, J. Bansmann, K. H. Meiwes-Broer, and M. Getzlaff, J. Phys. Condens. Matter **20**, 445005 (2008).
[13]K. Schouteden, A. Lando, E. Janssens, C. Van Haesendonck, and P. Lievens, New J. Phys. **10**, 083005 (2008).
[14]Z. Song, J. Hrbek, and R. Osgood, Nano Lett. **5**, 1327 (2005).
[15]D. V. Potapenko, J. Hrbek, and R. M. Osgood, ACS Nano **2**, 1353 (2008).
[16]J. A. Rodriguez, S. Ma, P. Liu, J. Hrbek, J. Evans, and M. Perez, Science **318**, 1757 (2007).
[17]E. Farfan-Arribas, J. Biener, C. M. Friend, and R. J. Madix, Surf. Sci. **591**, 1 (2005).
[18]M. S. Chen and D. W. Goodman, Catal. Today **111**, 22. (2006).
[19]R. E. Palmer, S. Pratontep, and H. G. Boyen, Nat. Mater. **2**, 443 (2003).
[20]N. Vandamme, E. Janssens, F. Vanhoutte, P. Lievens, and C. Van Haesendonck, J. Phys. Condens. Matter **15**, S2983 (2003).
[21]K. Schouteden, P. Lievens, and C. Van Haesendonck, Phys. Rev. B **79**, 195409 (2009).
[22]W. Bouwen, P. Thoen, F. Vanhoutte, S. Bouckaert, F. Despa, H. Weidele, R. E. Silverans, and P. Lievens, Rev. Sci. Instrum. **71**, 54 (2000).
[23]N. Ashcroft and N. Mermin, *Solid State Physics* (Holt, Rinehart and Winston, New York, 1976).
[24]J. Vangrunderbeek, C. Van Haesendonck, and Y. Bruynseraede, Phys. Rev. B **40**, 7594 (1989).
[25]C. Vlekken, Ph.D. thesis, K. U. Leuven, 1993.
[26]W. Chen, V. Madhavan, T. Jamneala, and M. F. Crommie, Phys. Rev. Lett. **80**, 1469 (1998).
[27]I. Horcas, R. Fernandez, J. M. Gomez-Rodriguez, J. Colchero, J. Gomez-Herrero, and A. M. Baro, Rev. Sci. Instrum. **78**, 013705 (2007).
[28]J. Biener, E. Farfan-Arribas, M. Biener, C. M. Friend, and R. Madix, J. Chem. Phys. **123**, 094705 (2005).
[29]S. Padovani, F. Scheurer, and J. P. Bucher, Europhys. Lett. **45**, 327 (1999).
[30]K. Schouteden, E. Lijnen, D. Muzychenko, A. Ceulemans, L. F. Chibotaru, P. Lievens, and C. Van Haesendonck, Nanotechnology **20**, 395401 (2009).
[31]F. Claeyssens, S. Pratontep, C. Xirouchaki, and R. E. Palmer, Nanotechnology **17**, 805 (2006).
[32]S. Narasimhan and D. Vanderbilt, Phys. Rev. Lett. **69**, 1564 (1992).
[33]H. Haberland, Z. Insepov, and M. Moseler, Phys. Rev. B **51**, 11061 (1995).
[34]S. J. Carroll, S. Pratontep, M. Streun, R. E. Palmer, S. Hobday, and R. Smith, J. Chem. Phys. **113**, 7723 (2000).
[35]P. Pyykkö, Inorg. Chim. Acta **358**, 4113 (2005).
[36]D. R. Lide, *CRC Handbook of Chemistry and Physics* (CRC Press, Boca Raton, Florida, 1993).
[37]P. E. Viljoen and J. P. Roux, Vacuum **41**, 1746 (1990).
[38]D. V. Potapenko and R. M. Osgood, Nano Lett. **9**, 2378 (2009).
[39]R. Berndt, J. K. Gimzewski, and R. R. Schlittler, Surf. Sci. **310**, 85 (1994).
[40]E. Dupont-Ferrier, P. Mallet, L. Magaud, and J. Y. Veuillen, Phys. Rev. B **75**, 205315 (2007).
[41]G. D. J. Smit, S. Rogge, and T. M. Klapwijk, Appl. Phys. Lett. **81**, 3852 (2002).
[42]R. T. Tung, Appl. Phys. Lett. **58**, 2821 (1991).
[43]Y. Yin, J. Jiang, Q. Cai, and B. Cai, Appl. Surf. Sci. **199**, 319 (2002).
[44]D. Matthey, J. G. Wang, S. Wendt, J. Matthiesen, R. Schaub, E. Laegsgaard, B. Hammer, and F. Besenbacher, Science **315**, 1692 (2007).
[45]K. Mitsuhara, Y. Kitsudo, H. Matsumoto, A. Visikovskiy, M. Takizawa, T. Nishimura, T. Akita, and Y. Kido, Surf. Sci. **604**, 548 (2010).
[46]E. Bertel and N. Memmel, Appl. Phys. A: Mater. Sci. Process. **63**, 523 (1996).
[47]N. Lopez, T. V. W. Janssens, B. S. Clausen, Y. Xu, M. Mavrikakis, T. Bligaard, and J. K. Nørskov, J. Catal. **223**, 232 (2004).
[48]B. Yoon, H. Hakkinen, U. Landman, A. S. Worz, J. M. Antonietti, S. Abbet, K. Judai, and U. Heiz, Science **307**, 403 (2005).